π- and σ-Coordinated Al in AlC_2^- and $AlCSi^-$. A Combined Photoelectron Spectroscopy and ab Initio Study

Alexander I. Boldyrev,*,†,‡ Jack Simons,*,† Xi Li,§ and Lai-Sheng Wang*,§

Contribution from the Department of Chemistry, The University of Utah, Salt Lake City, Utah 84112, Department of Chemistry and Biochemistry, Utah State University, Logan, Utah 84322-0300, Department of Physics, Washington State University, Richland, Washington 99352, and W. R. Wiley Environmental Molecular Sciences Laboratory, Pacific Northwest National Laboratory, MS K8-88, P.O. Box 999, Richland, Washington 99352

Received June 21, 1999

Abstract: Vibrationally resolved photoelectron spectroscopy is combined with ab initio calculations to investigate the structure and chemical bonding in AlC_2^- and $AlCSi^-$. AlC_2^- was found to have a C_{2v} structure whereas $AlCSi^-$ was found to be almost linear, thus establishing π-coordination of Al in AlC_2^- and σ-coordination in $AlCSi^-$. The adiabatic electron affinities of AlC_2 and AlCSi were measured to be 2.65(3) and 2.50(6) eV, respectively. The calculated vertical (2.87 eV) and adiabatic (2.60 eV) electron detachment energies for AlC_2^- agree well with the 2.73(0.03) and 2.65(0.03) eV experimental values, respectively. The calculated (2.86 eV) and experimental (2.64 ± 0.04 eV) vertical detachment energies for $AlCSi^-$ were also in good agreement. The calculated vibrational frequency for AlC_2 and vertical detachment energies for other higher energy features in both AlC_2^- and $AlCSi^-$ were also in good agreement with the experimental measurements. The combined experimental and theoretical effort allows us to elucidate the structures of AlC_2^- and $AlCSi^-$ and the nature of their chemical bonding.

Introduction

The −CC− group is known to bond to a variety of atoms and functional groups, such as H, F, and CH_3, using σ-coordination to produce linear X−C≡C−X neutral and X−C≡C$^-$ anion structures. However, when X is an electropositive atom such as Li, Mg, Al, Ti, etc., π-coordination is known to be more favorable.[1−8] Simple electrostatic models based on charge transfer from X to C_2 are used to explain why electropositive atoms prefer to form π-complexes. However, when one carbon atom is replaced by a more electropositive but isovalent atom such as silicon, it is not clear if the σ-complex of XCSi will be favored over the π-complex. In this work, we undertake a combined theoretical and experimental work on two anions AlC_2^- and $AlCSi^-$ which help address the question of the relative stabilities of σ- and π-coordination of electropositive aluminum to C_2^- and CSi^-. We found that indeed σ-coordination is favored in $AlCSi^-$, in contrast to AlC_2^-, where π-coordination occurs.

Experimental Methods

We used anion photoelectron spectroscopy (PES) to obtain electronic and vibrational information about AlC_2^-, $AlCSi^-$, and their respective neutral species. The experiments were carried out with a magnetic-bottle time-of-flight PES apparatus, equipped with a laser vaporization cluster source. Details of the experiment have been described previously.[9,10] AlC_2^- and $AlCSi^-$ were produced by laser vaporization of a graphite/Al or graphite/Al/Si composite target, respectively, with a pure helium carrier gas, and detected by a time-of-flight mass spectrometer. The anion species of interest were selected, decelerated, and photodetached with two photon energies: 355 (3.496 eV) and 266 nm (4.661 eV). Photoelectron time-of-flight spectra were measured and converted to electron binding energy spectra calibrated with the known spectrum of Cu^-. The electron kinetic energy resolution of the apparatus was typically 25 meV for 1 eV electrons.

Computational Methods

We initially optimized the geometries of AlC_2, AlC_2^-, AlCSi, and $AlCSi^-$ employing analytical gradients with polarized split-valence basis sets (6-311+G*)[11−13] using the hybrid method, which includes a mixture of Hartree−Fock exchange with density functional exchange-correlation (B3LYP).[14−16] Then, the geometries were refined using the CCSD(T)

† The University of Utah.
‡ Utah State University.
§ Washington State University and Pacific Northwest National Laboratory.

(1) (a) Apeloig, Y.; Schleyer, P. v. R.; Binkley, J. S.; Pople, J. A.; Jorgenson, W. L. *Tetrahedron Lett*. **1976**, 3973. (b) Disch, R. L.; Schulman, J. M.; Ritchie, J. P. *J. Am. Chem. Soc*. **1984**, *106*, 6246. (c) Schleyer, P. v. R. *J. Phys. Chem*. **1990**, *94*, 5560.
(2) (a) Ramondo, F.; Bencivenni, L.; Grandinetti, F. *J. Mol. Struct. (THEOCHEM)* **1990**, *206*, 205. (b) Ramondo, N.; Sanna, F.; Bencivenni, L. *J. Mol. Struct. (THEOCHEM)* **1992**, *258*, 361.
(3) Green, S. *Chem. Phys. Lett*. **1984**, *112*, 29.
(4) Boldyrev, A. I.; Simons, J. *J. Phys. Chem. A* **1997**, *101*, 2215.
(5) Knight, L. B., Jr.; Cobranchi, S. T.; Herlong, J. O.; Arrington, C. A. *J. Chem. Phys*. **1990**, *92*, 5856.
(6) Flores, J. R.; Largo, A. *Chem. Phys*. **1990**, *140*, 19.
(7) Sumathi, R.; Hendrickx, M. *Chem. Phys. Lett*. **1998**, *287*, 496.
(8) Li, X.; Wang, L. S. *J. Chem. Phys*. Submitted for publication. Wang, X. B.; Ding, C. F.; Wang, L. S. *J. Phys. Chem. A* **1997**, *101*, 7699.
(9) Wang, L. S.; Cheng, H. S.; Fan, J. *J. Chem. Phys*. **1998**, *102*, 9480.
(10) Wang, L. S.; Wu, H. In *Advances in Metal and Semiconductor Clusters. IV. Cluster Materials*; Duncan, M. A., Ed.; JAI Press: Greenwich, 1998; pp 299−343
(11) McLean, A. D.; Chandler, G. S. *J. Chem. Phys*. **1980**, *72*, 5639.
(12) Clark, T.; Chandrasekhar, J.; Spitznagel, G. W.; Schleyer, P. v. R. *J. Comput. Chem*. **1983**, *4*, 294.
(13) Frisch, M. J.; Pople, J. A.; Binkley, J. S. *J. Chem. Phys*. **1984**, *80*, 3265.
(14) Parr, R. G.; Yang, W. *Density-functional theory of atoms and molecules*; Oxford University Press: Oxford, 1989.
(15) Becke, A. D. *J. Chem. Phys*. **1992**, *96*, 2155.
(16) Perdew, J. P.; Chevary, J. A.; Vosko, S. H.; Jackson, K. A.; Pederson, M. R.; Singh, D. J.; Fiolhais, C. *Phys. Rev. B* **1992**, *46*, 6671.

10.1021/ja992102z CCC: $18.00
Published on Web 10/13/1999

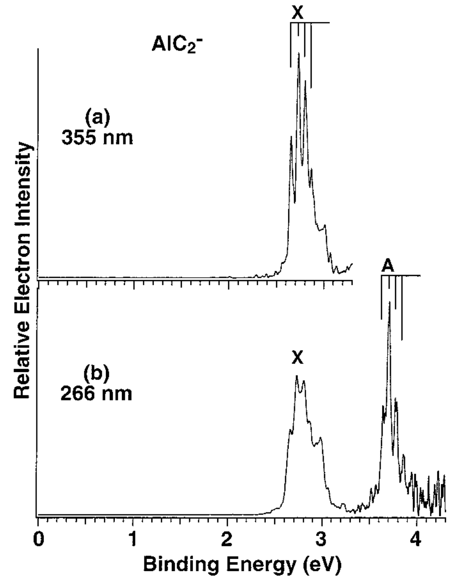

Figure 1. Photoelectron spectra of AlC_2^- at (a) 355 nm (3.496 eV) and (b) 266 nm (4.661 eV). The observed detachment channels are labeled (X and A). Vertical lines indicate vibrational progressions.

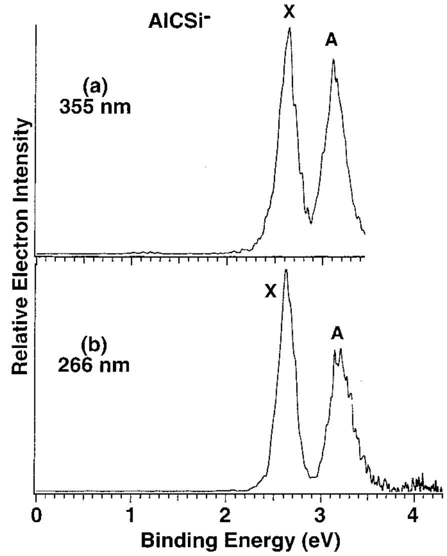

Figure 2. Photoelectron spectra of $AlCSi^-$ at (a) 355 nm (3.496 eV) and (b) 266 nm (4.661 eV). The observed detachment channels are labeled (X and A).

method[17−19] and the same basis sets. Finally, the energies of the lowest-energy structures were refined using the CCSD(T) level of theory and the more extended 6-311+G(2df) basis sets. All core electrons were kept frozen in treating the electron correlation at the CCSD(T) levels of theory. Vertical electron detachment energies from the lowest-energy singlet structures of AlC_2^- and $AlCSi^-$ were calculated using the outer valence Green function (OVGF) method[20−24] incorporated in Gaussian-94. The 6-311+G(2df) basis sets were used in all OVGF calculations, and all calculations were performed using the Gaussian-94 program.[25]

Experimental Results

Figure 1 shows the PES spectra of AlC_2^- at two wavelengths, 355 and 266 nm. The 355-nm spectrum revealed one band (X) that contains a well-resolved vibrational progression with a 590 cm^{-1} spacing. The 0−0 transition yields an adiabatic electron affinity (ADE) of 2.65 eV for AlC_2 while the strongest vibrational feature yields a vertical detachment energy (VDE) of 2.73 eV. A second detachment feature (A) was observed at 3.71 eV VDE, also with a well-resolved vibrational progression of 590 cm^{-1} spacing, similar to that in the X band.

Figure 2 displays the PES spectra of $AlCSi^-$ at the two detachment photon energies. The 355-nm spectrum shows two detachment features with VDEs at 2.64 (X) and 3.15 eV (A), respectively. However, no vibrational structures were resolved for either band of the $AlCSi^-$ spectrum. The 266-nm spectrum of $AlCSi^-$ revealed no additional detachment features. The adiabatic electron affinity of AlCSi was estimated from the onset of the X feature to be 2.50 eV, which is slightly smaller than that for AlC_2.

The spectra of AlC_2^- and $AlCSi^-$ are similar, except that the A-feature of $AlCSi^-$ has a considerably lower binding energy compared to that of the AlC_2^- spectrum. The measured electron detachment energies and spectroscopic constants for AlC_2 and AlCSi are summarized in Table 1.

Table 1. Observed Adiabatic (ADE) and Vertical (VDE) Detachment Energies for AlC_2^- and $AlCSi^-$ and the Obtained Spectroscopic Constants for AlC_2 and AlCSi

		ADE (eV)	VDE (eV)	term values (eV)	vib freq (cm^{-1})
AlC_2	X	2.65(3)	2.73(3)	0	590(40)
	A	3.63(4)	3.71(4)	0.98(4)	590(50)
AlCSi	X	2.50(6)	2.64(4)	0	
	A	3.02(8)	3.15(6)	0.52(8)	

Theoretical Results

AlC_2^-. At the B3LYP/6-311+G* level of theory, the global minimum of AlC_2^- was found to have a linear singlet $C_{\infty v}$ ($^1\Sigma^+$, $1\sigma^2 2\sigma^2 1\pi^4 3\sigma^2 4\sigma^2$) structure (characterized in Table 2). The cyclic C_{2v} ($^1A_1$, $1a_1^2 1b_2^2 2a_1^2 1b_1^2 3a_1^2 4a_1^2$) structure was found to be a local minimum only 1.4 kcal/mol higher in energy. However, at the higher CCSD(T)/6-311+G* level of theory, the $C_{\infty v}$ ($^1\Sigma^+$) linear structure is a second-order saddle point with the cyclic C_{2v} ($^1A_1$) structure being the global minimum (Table 2). The linear structure corresponds to a barrier on the intramolecular rotation of Al^+ around the C_2^{2-} group. The height of the internal rotation barrier is only 2.1 kcal/mol at the CCSD(T)/6-311+G(2df) level of theory.

AlC_2. At the B3LYP/6-311+G* level of theory, the global minimum of AlC_2 was found to have a cyclic C_{2v} ($^2A_1$, $1a_1^2 1b_2^2 2a_1^2 1b_1^2 3a_1^2 4a_1^1$) structure (Table 2). A linear singlet $C_{\infty v}$ ($^2\Sigma^+$, $1\sigma^2 2\sigma^2 1\pi^4 3\sigma^2 4\sigma^1$) structure was found to be a local minimum, 8.7 kcal/mol higher in energy. At the CCSD(T)/6-311+G* level of theory, the $C_{\infty v}$ ($^1\Sigma^+$) linear structure becomes a second-order saddle point while the cyclic C_{2v} ($^1A_1$)

(17) Cizek, J. *Adv. Chem. Phys.* **1969**, *14*, 35.
(18) Purvis, G. D., III; Bartlett, R. J. *J. Chem. Phys.* **1982**, *76*, 1910.
(19) Scuseria, G. E.; Janssen, C. L.; Schaefer, H. F., III *J. Chem. Phys.* **1988**, *89*, 7282.
(20) Cederbaum, L. S. *J. Phys.* **1975**, *B8*, 290.
(21) Niessen, W. von; Shirmer, J.; Cederbaum, L. S. *Comput. Phys. Rep.* **1984**, *1*, 57.
(22) Zakrzewski, V. G.; Niessen, W. von *J. Comput. Chem.* **1993**, *14*, 13.
(23) Zakrzewski, V. G.; Ortiz, J. V. *Int. J. Quantum Chem.* **1995**, *53*, 583.
(24) Ortiz, J. V.; Zakrzewski, V. G.; Dolgunitcheva, O. In *Conceptual Trends in Quantum Chemistry*; Kryachko, E. S., Ed.; Kluver: Dordrecht, 1997; Vol. 3, p 463.
(25) Frisch, M. J.; Trucks, G. W.; Schlegel, H. B.; Gill, P. M. W.; Johnson, B. G.; Robb, M. A.; Cheeseman, J. R.; Keith, T. A.; Peterson, G. A.; Montgomery, J. A.; Raghavachari, K.; Al-Laham, M. A.; Zakrzewski, V. G.; Ortiz, J. V.; Foresman, J. B.; Cioslowski, J.; Stefanov, B. B.; Nanayakkara, A.; Challacombe, M.; Peng, C. Y.; Ayala, P. Y.; Chen, W.; Wong, M. W.; Anders, J. L.; Replogle, E. S.; Gomperts, R.; Martin, R. L.; Fox, D. J.; Binkley, J. S.; DeFrees, D. J.; Baker, J.; Stewart, J. J. P.; Head-Gordon, M.; Gonzalez, C.; Pople J. A. *GAUSSIAN 94*, Revision A.1; Gaussian Inc.: Pittsburgh, PA, 1995.

Table 2. Calculated Molecular Properties of AlC_2^- and AlC_2

AlC_2^-, C_{2v}, $^1A_1$	B3LYP/6-311+G*	CCSD(T)/6-311+G*	AlC_2 C_{2v}, $^2A_1$	B3LYP/6-311+G*	CCSD(T)/6-311+G*
R(C−Al), Å	2.034	2.030	R(C−Al), Å	1.943	1.943
R(C−C), Å	1.263	1.283	R(C−C), Å	1.265	1.287
E_{tot}, au	−318.60875	−317.93499	E_{tot}, au	−318.51216	−317.84560
$\omega_1(a_1)$, cm^{-1}	1847	1770	$\omega_1(a_1)$, cm^{-1}	1798	1718
$\omega_2(a_1)$, cm^{-1}	579	595 cm^{-1}	$\omega_2(a_1)$, cm^{-1}	615	623
$\omega_3(b_2)$, cm^{-1}	105	129 cm^{-1}	$\omega_3(b_2)$, cm^{-1}	355	395
AlC_2^-, $C_{\infty v}$, $^1\Sigma^+$	B3LYP/6-311+G*	CCSD(T)/6-311+G*	AlC_2, $C_{\infty v}$, $^2\Sigma^+$	B3LYP/6-311+G*	CCSD(T)/6-311+G*
R(C−Al), Å	1.874	1.876	R(C−Al), Å	1.884	2.024
R(C−C), Å	1.265	1.281	R(C−C), Å	1.250	1.247
E_{tot}, au	−318.610935	−317.93108	E_{tot}, au	−318.49832	−317.82726
$\omega_1(\sigma)$, cm^{-1}	1922	1859	$\omega_1(\sigma)$, cm^{-1}	1843	1974
$\omega_2(\sigma)$, cm^{-1}	614	618	$\omega_2(\sigma)$, cm^{-1}	509	623
$\omega_3(\pi)$, cm^{-1}	114	145 i	$\omega_3(\pi)$, cm^{-1}	98	239 i

Table 3. Calculated Molecular Properties of $AlCSi^-$ and AlCSi

$AlCSi^-$, $C_{\infty v}$, $^1\Sigma^+$	B3LYP/ 6-311+G*	CCSD(T)/ 6-311+G*	$AlCSi^-$, C_s, $^1A'$	CCSD(T)/ 6-311+G*	AlCSi, $C_{\infty v}$, $^2\Sigma^+$	B3LYP/ 6-311+G*	CCSD(T)/ 6-311+G*
R(C−Al), Å	1.881	1.883	R(C−Al), Å	1.883	R(C−Al), Å	1.822	1.830
R(C−Si), Å	1.680	1.693	R(C−Si), Å	1.694	R(C−Si), Å	1.672	1.682
∠AlCSi, deg	180.0	180.0	∠AlCSi, deg	160.1	∠AlCSi, deg	180.0	180.0
E_{tot}, au	−570.04215	−568.97738	E_{tot}, au	−568.97759	E_{tot}, au	−569.94758	−568.88825
$\omega_1(\sigma)$, cm^{-1}	1258	1239	$\omega_1(a')$, cm^{-1}	1223	$\omega_1(\sigma)$, cm^{-1}	1251	1257
$\omega_2(\sigma)$, cm^{-1}	485	485	$\omega_2(a')$, cm^{-1}	514	$\omega_2(\sigma)$, cm^{-1}	509	509
$\omega_3(\pi)$, cm^{-1}	91	93 i	$\omega_3(a')$, cm^{-1}	74	$\omega_3(\pi)$, cm^{-1}	63	100 i

structure remains the global minimum (Table 2). This structure was also found to be the global minimum in previous ab initio calculations[5,6] as was established experimentally.[5] The linear structure represents a barrier on the intramolecular rotation Al^+ around the C_2^- group. The height of the internal rotation barrier is 12.3 kcal/mol at the CCSD(T)/6-311+G(2df) level of theory.

The calculated vertical and adiabatic electron detachment energies for AlC_2^- were found to be the following: VDE = 2.87 eV (OVGF/6-311+G(2df)) and ADE = 2.60 eV (CCSD(T)/6-311+G(2df)). Both AlC_2^- and AlC_2 are very stable thermodynamically with dissociation energies calculated to be the following: $\Delta E = 4.52$ eV for AlC_2^- (C_{2v}, $^1A_1$) → C_2^- ($D_{\infty h}$, $^2\Sigma_g^+$) + Al (^{2}P) and $\Delta E = 5.06$ eV for AlC_2 (C_{2v}, $^2A_1$) → C_2 ($D_{\infty h}$, $^1\Sigma_g^+$) + Al (^{2}P) (all at the CCSD(T)/6-311+G(2df) level of theory).

$AlCSi^-$. At the B3LYP/6-311+G* level of theory, the global minimum of $AlCSi^-$ was found to have a linear singlet $C_{\infty v}$ ($^1\Sigma^+$, $1\sigma^2 2\sigma^2 3\sigma^2 1\pi^4 4\sigma^2$) structure (characterized in Table 3). Alternative linear singlet $AlSiC^-$ $C_{\infty v}$ ($^1\Sigma^+$, $1\sigma^2 2\sigma^2 3\sigma^2 1\pi^4 4\sigma^2$) structure was also optimized at the B3LYP/6-311+G* level of theory, and it was found to be a second-order saddle point 60.8 kcal/mol higher in energy than the global minimum and it was excluded from further examination. The cyclic C_s ($^1A'$, $1a'^2 2a'^2 3a'^2 4a'^2 1a''^2 5a'^2$) structure collapsed into the $AlCSi^-$ $C_{\infty v}$ ($^1\Sigma^+$) structure upon geometry optimization. However, at the CCSD(T)/6-311+G* level of theory, the $C_{\infty v}$ ($^1\Sigma^+$) linear structure becomes a second-order saddle point, and a bent C_s ($^1A'$) structure becomes the global minimum (Table 3). The bent structure of $AlCSi^-$ is very different from the global minimum cyclic structure of AlC_2^- because it does not have a Al−Si bond and the AlCSi angle is 160° compared to the AlCC angle of 72° in AlC_2^-. A similar bent structure was found to be the global minimum for the isoelectronic neutral molecule SiCSi.[26−31] The energy required for linearization of $AlCSi^-$ is only 0.132 kcal/mol, which is comparable to the difference in ZPE corrections (0.124 kcal/mol) between the linear and bent structures (all at the CCSD(T)/6-311+G* level of theory). Therefore, $AlCSi^-$ has a nearly linear equilibrium structure, especially when zero-point vibrational motion is considered.

The $AlCSi^-$ anion is also very stable toward dissociation. The dissociation energy was calculated to be $\Delta E = 4.26$ eV for $AlCSi^-$ (C_{2v}, $^1A_1$) → CSi^- ($C_{\infty v}$, $^2\Sigma^+$) + Al (^{2}P) (at the CCSD(T)/6-311+G(2df) level of theory).

AlCSi. At the B3LYP/6-311+G* level of theory, the global minimum of AlCSi was found to have a linear doublet $C_{\infty v}$ ($^2\Sigma^+$, $1\sigma^2 2\sigma^2 3\sigma^2 1\pi^4 4\sigma^1$) structure, but this becomes a second-order saddle point at the CCSD(T)/6-311+G* level of theory. According to Koopmans' theorem, the 1π-MO is very close in energy to the 4σ-HOMO in $AlCSi^-$. Therefore we also optimized the geometry of another linear doublet $C_{\infty v}$ ($^2\Pi'$, $1\sigma^2 2\sigma^2 3\sigma^2 1\pi^3 4\sigma^2$) structure at the CCSD(T)/6-311+G* level of theory. This state was found to be linear, but 0.25 eV higher in energy than the $C_{\infty v}$ ($^2\Sigma^+$, $1\sigma^2 2\sigma^2 3\sigma^2 1\pi^4 4\sigma^1$) linear structure (Table 3) and therefore not the global minimum for AlCSi. Unfortunately, because the two $C_{\infty v}$ ($^2\Sigma^+$, $1\sigma^2 2\sigma^2 3\sigma^2 1\pi^4 4\sigma^1$) and $C_{\infty v}$ ($^2\Pi'$, $1\sigma^2 2\sigma^2 3\sigma^2 1\pi^3 4\sigma^2$) states are so close in energy, we were not able to complete the geometry optimization at the CCSD(T)/6-311+G* level of theory at bent geometries due to convergence problems. We therefore were unable to calculate the adiabatic electron detachment energy of $AlCSi^-$.

In all four species studied here, the B3LYP method predicted a minimum in the linear configuration that is not preserved in the CCSD(T) calculations. We believe that the artificial minima for the linear configuration are essentially due to the one-configurational nature of the B3LYP method. One needs to use methods beyond the one-configurational approximation, such as CCSD(T) used here, to get reliable results for the species studied here.

(26) Weltner, E., Jr.; Mcleod, D., Jr. *J. Chem. Phys.* **1964**, *41*, 235.
(27) Kafafi, Z. H.; Hauge, R. H.; Fredin, L.; Margrave, J. L. *J. Phys. Chem.* **1983**, *87*, 797.
(28) Presilla-Marquez, J. D.; Graham, W. R. M. *J. Chem. Phys.* **1991**, *95*, 5612.
(29) Grev, R. S.; Schaefer, H. F., III *J. Chem. Phys.* **1985**, *82*, 4126.
(30) Rittby, C. M. L. *J. Chem. Phys.* **1991**, *95*, 5609.
(31) Bolton, E. E.; DeLeeuw, B. J.; Fowler, J. E.; Grev, R. S.; Schaefer, H. F., III *J. Chem. Phys.* **1992**, *97*, 5586.

Table 4. Comparison of Calculated and Experimental Electron Detachment Processes of AlC_2^-

C_{2v}, $^1A_1$ state	expt VDE (eV)	expt ADE (eV)	electron detachment from MO	theory VDE[a] (eV)	theory, ADE[b] (eV)	$C_{\infty v}$, $^1\Sigma^+$ state	electron detachment from MO	theory VDE[a] (eV)
X	2.73(3)	2.65(3)	$4a_1$	2.87(0.90)	2.60	X	4σ	3.54(0.89)
A	3.71(4)	3.63(4)	$3a_1$	3.64(0.87)		A	1π	3.99(0.88)

[a] Pole strength is given in parentheses. [b] At the CCSD(T)/6-311+G(2df) level of theory using CCSD(T)/6-311+G* geometry.

Table 5. Comparison of Calculated and Experimental Vertical Electron Detachment Energies (VDE) of AlCSI$^-$

C_s, $^1A'$ state	exptl VDE (eV)	electron detachment from MO	theory VDE[a] (eV)
X	2.64(4)	5a′	2.86(0.88)
A	3.15(6)	1a″	3.01(0.88)
		4a′	3.00(0.88)

Interpretation of the Experimental Spectra

AlC_2^-. In Table 4 we present the results of our calculations of the two major low-lying vertical one-electron detachment processes from the cyclic C_{2v} ($^1A_1$) state of AlC_2^-.

Feature X. The lowest vertical electron detachment occurs by electron removal from the $4a_1$-HOMO. The feature X (Figure 1) peaking at 2.73 ± 0.03 eV agrees well with the calculated VDE of 2.87 eV [OVGF/6-311+G(2df)] from the $4a_1$-HOMO. The 355-nm spectrum revealed a well-resolved vibrational progression with a 590-cm^{-1} spacing. According to our calculations, the main change in geometry upon electron detachment of AlC_2^- occurs in the Al−C distance, which is 0.087 Å shorter in the neutral AlC_2. Therefore, one expects a vibrational progression due to the Al−C_2 stretching mode in the PES spectrum of AlC_2^-. The calculated value for the frequency of this vibration (ν_2 in Table 2) is in good agreement with the experimentally observed vibrational spacing of 590 cm^{-1}, considering the large uncertainty of the measured value. The 0−0 transition yields an adiabatic electron affinity of 2.65 eV for AlC_2 that again agrees well with the calculated value of 2.60 eV (CCSD(T)/6-311+G(2df)).

Feature A. The second vertical electron detachment from the $3a_1$-(HOMO-1) should occur at 3.64 eV (OVGF/6-311+G(2df)) (Table 4). This value agrees well with the second detachment feature (A), which was observed at 3.71 eV. Unfortunately, the CCSD(T) method is not suitable for calculations of excited states having the same symmetry as the lower states, so we were not able to calculate the geometry relaxation and frequencies for the first excited state of AlC_2. We were able to calculate the vertical detachment energy because of the OVGF method used.

In Table 4 we also present the calculated electron detachment energies for the linear AlC_2^- $C_{\infty v}$ ($^1\Sigma^+$, $1\sigma^2 2\sigma^2 1\pi^4 3\sigma^2 4\sigma^2$). It is clear that these VDEs do not agree nearly as well with the experimental PES spectra. We therefore conclude that both AlC_2^- and AlC_2 have the cyclic C_{2v} structures based on our calculations and experimental data.

AlCSi$^-$. In Table 5 we present the results of our calculations of the two major low-lying vertical one-electron detachment processes from the slightly bent C_s ($^1A'$) state of AlCSi$^-$.

Feature X. The lowest vertical electron detachment occurs by electron removal from the 5a′-HOMO. The feature X (Figure 1) peaking at 2.64 ± 0.04 eV is in reasonable agreement with the calculated VDE of 2.86 eV [OVGF/6-311+G(2df)] from the 5a′-HOMO. There were discernible vibrational structures in the X-feature, which was probably due to the C−Al stretching. However, the bending mode, which has a very low frequency (Table 3), was probably also active, resulting in the broad and unresolved feature.

Feature A. The second vertical electron detachment from the very closely spaced 1a″-MO or 4a′-MO (which are almost degenerate because they originate from the 1π-HOMO in the linear structure) occurs at 3.01 eV (OVGF/6-311+G(2df)). This value agrees well with the second detachment feature (A), observed at 3.15 ± 0.06 eV. The 266-nm spectrum revealed a splitting in the second peak, which might derive from the quasidegeneracy of the 1a″ and 4a′ MO found in our calculations. We therefore conclude that both AlCSi$^-$ and AlCSi have quasilinear structures based on our calculations and the experimental data.

Discussion

The overall agreement between the experimental PES spectra and the theoretical calculations is quite satisfying. In particular, the excellent agreement between the calculations and the experimentally observed peak X in AlC_2^- provides strong support for the cyclic structure with π-coordination of aluminum to C_2 in AlC_2^- and in AlC_2. The cyclic structure of AlC_2 was previously found in ab initio calculations[5,6] and in rare gas matrix electron spin resonance studies by Knight and others.[5]

The agreement between the calculations and observed PES spectral features of the AlCSi$^-$ anion provides strong support for the quasilinear structure with σ-coordination of aluminum in AlCSi$^-$ and in AlCSi. The vertical and adiabatic electron detachment energies are also very high for the AlCSi$^-$ anion (Table 1) and they can be explained in the same fashion as in the AlC_2^- anion. Surprisingly, both VDE and ADE of AlCSi$^-$ are very close to the corresponding values in AlC_2^-, despite the fact that one carbon was substituted by a more electropositive silicon atom. On the other hand, one should take into account the fact that AlCSi$^-$ has σ-coordination, while AlC_2^- has π-coordination. If we compare the σ-complexes for both anions, VDE(AlC_2^-) = 3.54 eV and VDE(AlCSi$^-$) = 2.86 eV, one can see a substantial reduction in electron binding energy in AlCSi$^-$. Simple electrostatic considerations can also help to understand why AlC_2^- has π-complex structure, while AlCSi$^-$ has σ-complex structure. Although the effective atomic charges in both anions show a high degree of ionicity, the two carbon atoms have the same charges in the cyclic AlC_2^-, whereas in AlCSi$^-$ the carbon carries a larger negative charge than silicon, which favors the σ-complex configuration in the latter.

Conclusions

We report a combined experimental and theoretical investigation of AlC_2^- and AlCSi$^-$ and their corresponding neutrals. Photoelectron spectra of the anions were measured and the electron detachment energies and vibrational frequencies were obtained. The adiabatic electron affinities of AlC_2 and AlCSi were determined to be 2.65(3) and 2.50(6) eV, respectively. The first electronic excited state was also observed for each species. Our theoretical calculations predicted that AlC_2^- and AlC_2 both have a C_{2v} cyclic structure while AlCSi$^-$ and AlCSi have quasilinear structures. The agreement between the calculated and experimental spectroscopic parameters confirms the π-coordination of Al in AlC_2^- and σ-coordination of Al in $AlCSi^-$.

Acknowledgment. The theoretical work done in Utah is supported by the National Science Foundation (CHE-9618904). The authors acknowledge the Center for High Performance Computations at the University of Utah for computer time. The experimental work done in Washington is supported by the National Science Foundation (DMR-9622733). The experiment was performed at the W. R. Wiley Environmental Molecular Sciences Laboratory, a national scientific user facility sponsored by DOE's Office of Biological and Environmental Research and located at Pacific Northwest National Laboratory, which is operated for DOE by Battelle under Contract DE-AC06-76RLO 1830. L.S.W. is an Alfred P. Sloan Foundation Research Fellow.

JA992102Z